

# **Fe<sup>3+</sup>/Fe<sup>2+</sup> - ZnO nanostructures: Synergetic effect of annealing temperature on Structural, Optical and Dielectric properties**

Anil Kaushik\*, Sunil Kumar Chaudhary†, Ajay Kumar Mann‡

## **Abstract**

The impact of Fe<sup>3+</sup> dopant on structural, morphological and electric properties of ZnO nano materials prepared via co-precipitation methodology is explored in this work. The XRD measurements affirmed the wurtzite hexagonal arrangement with the P63mc space group. Crystalline size, inter-planar spacing, and cell volume of the Fe<sup>3+</sup>/ZnO-400 were determined to be 38.6 nm, 2.6903 nm and 57.44 Å<sup>3</sup>, individually. SEM (Scanning Electron Microscope) was utilized for morphological investigations of the surface of samples. The photoluminescence (PL) studies were estimated at 325 nm excitation wavelength via utilizing a photoluminescence spectrometer to observe the emission spectrum of samples. FTIR (Fourier Transform Infrared) spectrometer was used to measure IR spectra to identify the presence of bonds in the samples with peaks around 536-634 cm<sup>-1</sup>. Complex impedance measurements of the Fe<sup>3+</sup>/ZnO-RT and Fe<sup>3+</sup>/ZnO-400 samples were estimated at 310 K using a galvanostat in the range of frequency from 50 Hz to 5 MHz.

---

\* Department of Physics, Baba Masnath University, Rohtak, Haryana, India; [gphysics07@gmail.com](mailto:gphysics07@gmail.com)

† Department of Physics, Baba Masnath University, Rohtak, Haryana, India; [sunilkc2001in@yahoo.com](mailto:sunilkc2001in@yahoo.com)

‡ Department of Physics, Pandit Neki Ram Sharma Government College, Rohtak, Haryana, India; [mannajay77@gmail.com](mailto:mannajay77@gmail.com)

**Keywords:** Fe<sup>3+</sup>/Fe<sup>2+</sup>, Doped Zinc Oxide, SEM, Photoluminescence, FTIR, Complex Impedance

## 1. Introduction

Nanomaterials made of metal oxides have exceptional structural, optical and electrical characteristics. Because of its broadband gap ( $E_g=3.1-3.80$  eV) and widespread application in photovoltaic, catalyst, mechanical and spintronic fields, ZnO has received too much attention for a few decades [1, 2]. Numerous preparation methodologies, like co-precipitation, sol-gel, hydro-thermal and thermal evaporation were primarily utilized for the synthesis of ZnO or doped Zinc Oxide nano materials. From these techniques, the co-precipitation process is mostly exploited for the preparation of ZnO (from II-VI group) nano materials in vast passable extents and crouchexpense as per required industrialized relevances. Rocksalt, Zinc blende and wurtzite are three crystalline forms of zinc oxide. As a result, under ubiquitous conditions, the hexagonal wurtzite from the P63mc space group is the primary stable phase [3]. The Zinc atoms were tetrahedrally synced to oxygen atoms in the Zinc Oxide crystals and the Zinc 3d electrons hybridized with the 3p electrons of the oxygen atoms [4]. There are various ways of further developing the functional properties of ZnO, for example, modifying the dimension and state of Zinc Oxide or doping with metal (Al, Fe, Mg, etc) or non-metals atom on the A-site of Zinc Oxide [5, 6]. Doping with metal or non-metal oxides has demonstrated to be a fruitful strategy for making interesting structures with customized physical and elemental behaviour (like structure, electronic, and catalytic characters) with many potential applications [7]. M. Maniknandan et al., reported the work on Sn doped ZnO for piezoelectric applications [8]. A. Akdaq et al., published the work on structural and morphological properties of Al substituted ZnO [9]. Y. Yang et al., reported a review work on ZnO-based nano materials for various applications [10]. Besides, nano materials doped with trivalent metal atoms/rare earth atoms on the Zn-site of ZnO are drawing coherent attention because of their large industrialized relevance in catalysis, iridescence, and electronics, and in various other fields [8]. In this work, we studied the consequence of annealing on structural, optical, morphological,

and electrical characteristics of Fe<sup>3+</sup> tailored Zinc Oxide synthesized via a co-precipitation approach.

## 2. Experimental Details

### 2.1. Chemicals & Synthesis Procedure

Zn(CH<sub>3</sub>COO)<sub>2</sub>, Na-OH (Sodium-Hydroxide), Fe(NO<sub>3</sub>)<sub>3</sub>·9H<sub>2</sub>O (Iron nitrate), C<sub>2</sub>H<sub>5</sub>OH (Ethanol), and DI water were used as early ingredients to manufacture Loba in this study, and no further refinement was required. The initial ingredients were used in a stoichiometric quantity of Zn(CH<sub>3</sub>COO)<sub>2</sub> and Na-OH in the straight co-precipitation preparation of Fe<sup>3+</sup> tailored ZnO nano materials (shortened Fe<sup>3+</sup>/ZnO at 300 K & Fe<sup>3+</sup>/ZnO at 400 ° C). The ingredients were that mixed in a solution of C<sub>2</sub>H<sub>5</sub>OH and DI water. The solution of these preface components is then stimulated for 2 h at 353 K. This mixture was kept to sit all night and cleaned numerous moments with DI water since being desiccated in an oven for 12 hr at 363 K. As a consequence, the prepared sample was kept in the furnace at 400 °C for 2 hours.

### 2.2. Characterizations

Using XRD (Rigaku's XRD) (with a radiation source of Cu-K $\alpha$ ;  $\lambda$  = 1.542Å), the space group and crystal configuration of manufactured Fe<sup>3+</sup>/ZnO-RT and Fe<sup>3+</sup>/ZnO-400 materials were studied. The scanning angle of diffraction varied from 10° to 90° with a scan speed of 2° per min. The SEM was utilized to explore the surface morphologies and EDS with 20 kV accelerating voltage of the Fe<sup>3+</sup>/ZnO-RT and Fe<sup>3+</sup>/ZnO-400 materials. A PL spectrometer was utilized to decide the energy gap and emissions spectrum. The FT-IR was utilized to observe the stretching of bonds in ZnO materials. Galvanostat (SP240; Bio Logic) was used to investigate AC impedance.

## 3. Results and discussions

### 3.1. XRD Analysis

Figure 1 revealed XRD measurements of well prepared Fe<sup>3+</sup>/ZnO-RT and Fe<sup>3+</sup>/ZnO-400 nano materials of Fe<sup>3+</sup>-tailored Zinc Oxide in a range of 10° to 90°. The peaks of diffraction at  $2\theta$  values of 31.76, 34.29, 36.28, 47.58, 56.35, 62.57, 67.96, 69.13, 72.49, 77.01 and 81.55 consequent to various hkl values (100), (002), (101), (102), (110),

(103), (200), (112), (201) and (202), correspondingly. JCPDS #80-0075 was used to verify all of the obtained XRD peaks. Debye Scherer's relation [8] could be applied for estimation of the average value of grain size (D):

$$D = 0.9\lambda / \beta \cos\theta \dots\dots\dots (1)$$

Where,  $\lambda = 1.542 \text{ \AA}$  (X-ray wavelength),  $\beta(hkl)$  = full width along half maxima (FWHM),  $\theta$  = Bragg's angle.

The law of Bragg was used to determine the inter-planar spacing ( $d_{hkl}$ ) of the ZnO based samples, which were deliberated as:

$$2d_{hkl}\sin\theta = n\lambda \dots\dots\dots (2)$$

Where 'n' is the array of diffractions,  $\lambda = 1.542 \text{ \AA}$  (X-ray's wavelength) and  $\theta$  = diffraction angles.

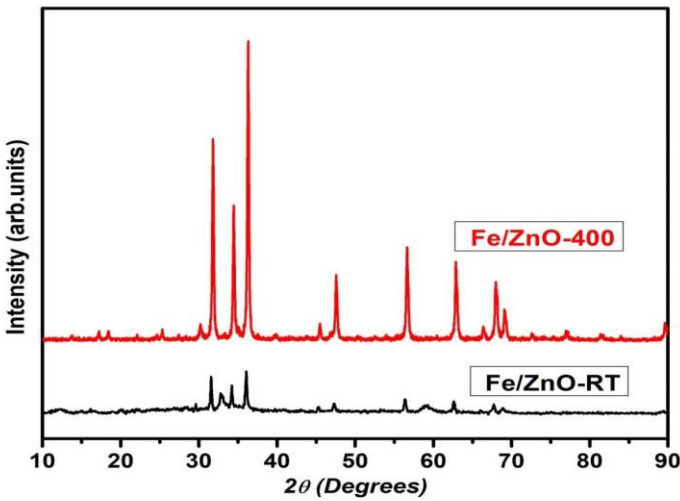


Fig. 1. XRD patterns of  $Zn_{0.92}Fe_{0.08}O$  at 300 K ( $Fe^{3+}/ZnO-RT$ ) and annealed at  $400 \text{ }^\circ C$  ( $Fe^{3+}/ZnO-400$ ).

The crystal variables and cell volume of the manufactured  $Fe^{3+}/ZnO-RT$  &  $Fe^{3+}/ZnO-400$  nano materials were estimated as:

$$a = d_{hkl} * \sqrt{h^2 + k^2 + l^2} \dots\dots\dots (3)$$

$$V = \frac{\sqrt{3}}{2} * a^2 * c \dots\dots\dots(4)$$

Where  $d_{hkl}$  is the inter-planer spacing, (hkl) is the millers indices of the corresponding planes and a & c are the crystal constants. The derived variables are listed in table no. 1.

**Table 1.** XRD parameter of Fe<sup>3+</sup> doped ZnO

Samples	Grain size (nm)	Inter-planar spacing ( $d_{hkl}$ )Å	lattice constant(Å)		Volume (V) of Cell (Å <sup>3</sup> )
			a = b	C	
Fe <sup>3+</sup> /ZnO-400	36.8	2.6903	3.5538	5.3194	057.44
Fe/ZnO-RT	39.0	2.6663	3.5902	5.4121	061.38

### 3.2 Morphological Analysis

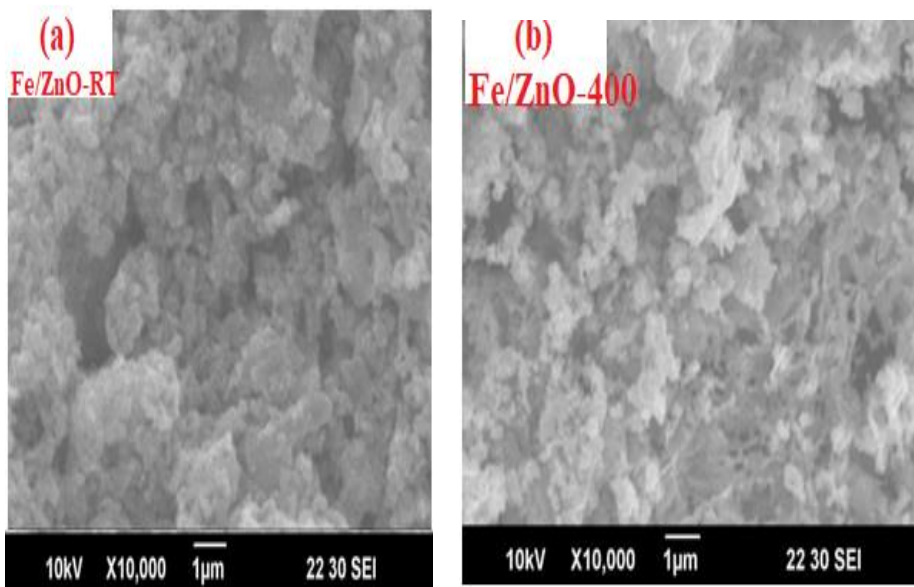


**Fig. 2 (a-b):** SEM images of (a) Fe<sup>3+</sup>/ZnO- RT (b) Fe<sup>3+</sup>/ZnO- 400 nanomaterials.

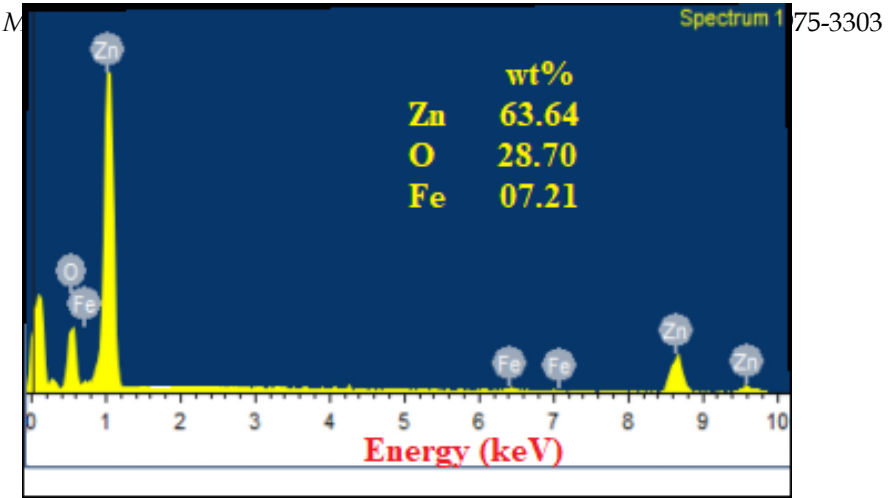


**Fig. 2 (c):** EDS spectra of Fe/ZnO-400 nanomaterial.

The SEM images are polycrystalline in appearance and indicate agglomeration, irregular forms, and sizes because of the massive chemical effect in the samples. The structural, electrical and many other properties of the nanostructures could be protected by the asymmetrical distribution of nano particles. This type of result could be due to their inferior diffusivities. With the XRD studies, the results are far too consistent. EDS was used to determine the chemical composition of Fe<sup>3+</sup>/ZnO-400 samples, as shown in Fig. 2 (c). The presence of strange peaks for Zn, Fe, and O validates the chemical composition of the synthesized material. There is a minor weight (wt %) percentage difference due to gold (Ag) coating during SEM measurements.

#### 4. PL Analysis

Figure 3 reveals the PL spectrum of Fe<sup>3+</sup>/ZnO-RT and Fe<sup>3+</sup>/ZnO-400) nano materials at an excitation wavelength ( $\lambda$ ) of 325 nm. There was strapping emission peak focused at 433.7 nm and 552.4 nm, thus was a red shift when contrasted with the close band emissions in pure Zinc Oxides. The Fe<sup>3+</sup> ions fashioned deficiencies in substituted ZnO, thus might foster trifling energy altitudes near the conduction edge.

Because of the fashioned trifling energy level, the violet emanation pinnacle may be ascribed to the recombination places [9]. Moreover, Zinc atoms interstitial and O opportunities were

generated in conjunction with the adaptation of Fe<sup>3+</sup>, thus significantly influencing the optical qualities of the altered ZnO tests with substituting atoms.

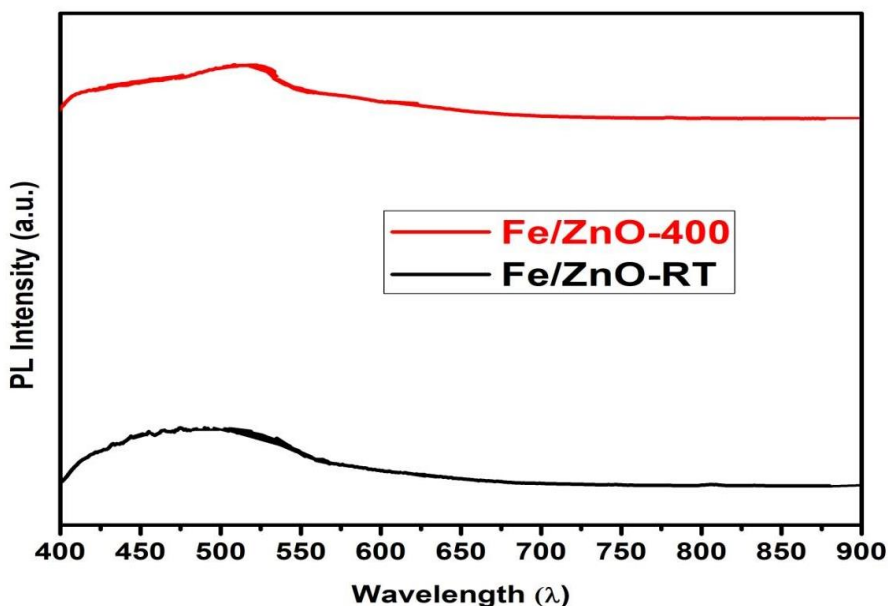


Fig. 3. PL spectra of Fe<sup>3+</sup>/ZnO-RT and Fe<sup>3+</sup>/ZnO-400 nanomaterials.

## 5. FTIR Studies

Figure 4 depicts the IR spectrum of Fe<sup>3+</sup>/ZnO-RT & Fe<sup>3+</sup>/ZnO-400) samples with wave numbers ranging from 500 to 3700 cm<sup>-1</sup>. The trembling of the C-H, O-H, and C-O or C=O bonds is characterized by the FTIR crest, which ranges from 675 to 1655 cm<sup>-1</sup>. The defect positions close to Fe<sup>3+</sup> atoms in the ZnO crystal are revealed via the diminutive and messy absorption edges near 830 cm<sup>-1</sup>. The stretch of Zn-O bonds is characterized through FTIR crests among 536-634 cm<sup>-1</sup> [10].

The residual FTIR crests, thus extent from 1750 to 3350 cm<sup>-1</sup> show the stretching quiverings of O-H bonds, the charisma of O=C=O bonds, and the bending mode of submerged water this is because of quenchable/annealing effects on Fe<sup>3+</sup>/ZnO nano materials,

which increases the crystallinity temperament of  $\text{Fe}^{3+}/\text{ZnO}$  and differentiation in morphologies of  $\text{Fe}^{3+}/\text{ZnO}$ , as evidenced by the X-RD data or SEM images of  $\text{Fe}^{3+}/\text{ZnO-400}$  nano materials.

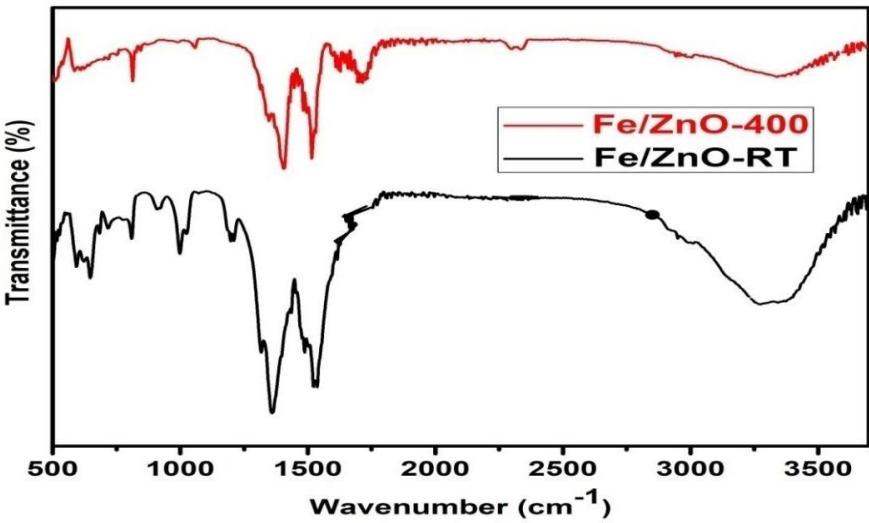


Fig. 4. IR Spectra of  $\text{Fe}^{3+}/\text{ZnO-RT}$  and  $\text{Fe}^{3+}/\text{ZnO-400}$  nano materials.

## 6. Impedance Spectroscopy (CIS) studies:

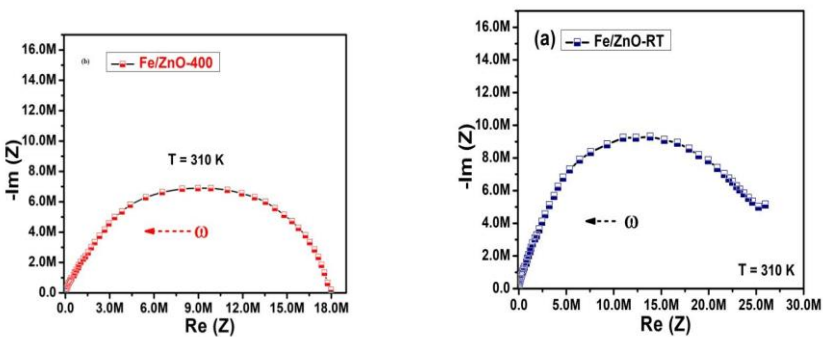


Fig. 5: Nyquist plots of (a) $\text{Fe}^{3+}/\text{ZnO-RT}$ (b) $\text{Fe}^{3+}/\text{ZnO-400}$  nanomaterials at room temperature (310 K).

The AC impedance spectroscopy is an admired practice for establishing the correlation between electronic transportation character and the structure of samples, also presenting knowledge on the scenery of electronic positions. Figure 5 (a-b) reveals the impedance ( $Z' + iZ''$ ) character or nyquist plots of Fe<sup>3+</sup>/ZnO-RT and Fe<sup>3+</sup>/ZnO-400 samples at room temperature (at 310 K) at a variety of frequencies (50 Hz - 05 MHz) (at 100 mV applied field).

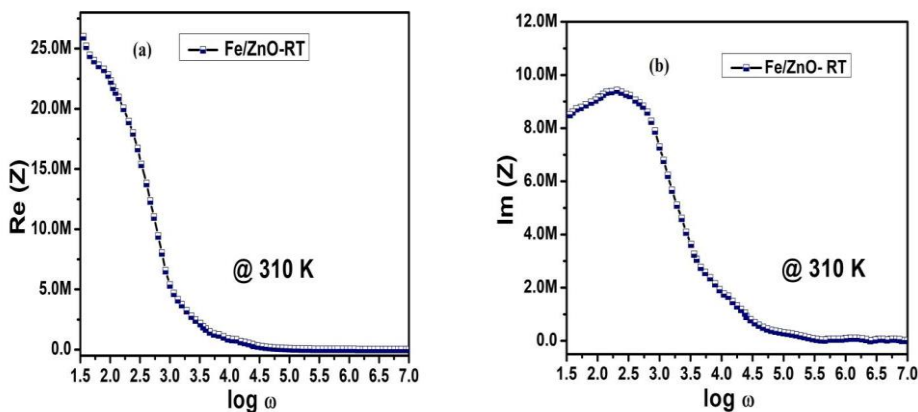


Fig. 6 (a) Plot of the Real part ( $Z'$ ) (b) Plot of Imzpart ( $Z''$ ) of impedance with frequencies for ZnO-RT sample.

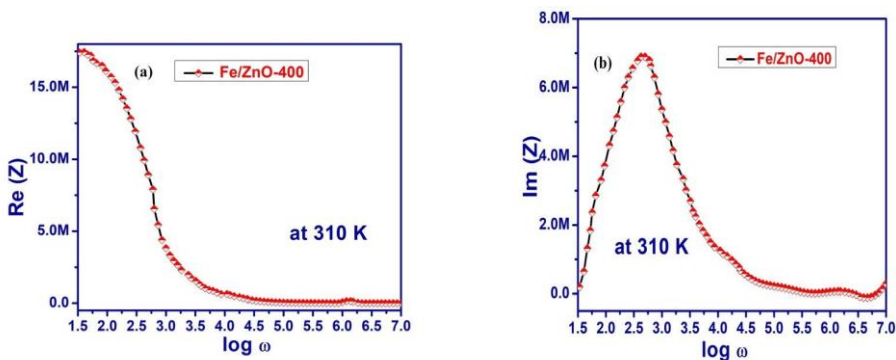


Fig. 7 (a) Plot of Real part ( $Z'$ ) (b) Plot of Imzpart ( $Z''$ ) of impedance with frequencies for ZnO-400 sample.

The AC impedance ( $Z$ ) can be calculated using the following formula:

$$Z = Z' - iZ'' \dots\dots\dots(5)$$

In this,  $Z'$  is the real fraction and  $Z''$  is the imag. fraction of AC impedance. To determine the electric convey behaviour of invisible light for the  $Fe^{3+}/ZnO-RT$  and  $Fe^{3+}/ZnO-400$  nano materials, the impedance spectrum was measured in a dark. The muddled impedance arcs add a different crescent bend, which is regularly brought about by the grain periphery [11, 12]. At 310 K, the semicircle arcs recommend a huge insulating characteristic. Besides, dielectric behaviour in the lower frequency range is connected to grain edge association, while relaxation behaviour at higher frequencies is connected with grain commitment. Thermally enacted accuse charges with superior energy defeats the protecting grain line and adds to electric conduction in semiconductor materials, bringing about this sort of action. The semicircles in the Cole-Cole plots show double variants of the dielectric relaxations phenomenon or non-Debye types behaviour [11]. In addition, at 310 K, figure 6 (a) and figure 7 (a) depict the transformation of the  $Z'$  of complex impedance with frequency task distinction for  $Fe^{3+}/ZnO-RT$  and  $Fe^{3+}/ZnO-400$ , respectively. It can be seen that magnitude of  $Z$  abruptly decreases with frequency function variation, indicating that this is because enlargement in AC conductivities cause the hopping conduction mechanism [13]. It is clear that, the  $Z'$  of complex impedance has thorny frequencies dependant behaviour in the inferior frequencies zone, hence communicating to elevated resistivities and larger grain periphery resistance value, while  $Z'$  behaves like a frequency monarch in the high-frequency domain. Furthermore, figure 6 (b) and figure 7 (b) illustrate the changing of imaginary fraction ( $Z''$ ) of impedance with frequency, demonstrating a behaviour that is quite similar to  $Z'$  for  $Fe^{3+}/ZnO-RT$  and  $Fe^{3+}/ZnO-400$ , respectively. Complex impedance results are used to identify the crystal arrangement in form of grain and grain edge, which correspond to the inferior and superior frequency dispersion zones [11, 13].

## 7. Conclusion

The Fe<sup>3+</sup> ion modified ZnO (called Fe<sup>3+</sup>/ZnO-RT and Fe<sup>3+</sup>/ZnO-400) nano materials were fruitfully synthesized through coprecipitation technique at diverse sintering temperatures to explore the influence of temperature on material synthesis and assorted properties. The wurtzite hexagonal arrangement with P<sub>6</sub>mc space group was demonstrated by X-RD (X-Ray Diffractions) outcomes. The crystalline size, intra-plane spacing, and dimensions of the cell for the Fe<sup>3+</sup>/ZnO-400 nano materials were estimated to be 36.8 nm, 2.6903nm and 57.44Å<sup>3</sup> correspondingly. SEM measurements revealed the agglomeration in the samples. The EDS measurements confirmed the elemental presence in the sample in stoichiometric amounts. The photoluminescence spectra were shows the sturdy emission peak focused at 433.7 nm and 552.4 nm, which has a red swing in contrast to the close band emissions in Zinc Oxide. From the IR spectra, it was observed that peaks around 536-634 cm<sup>-1</sup> as a result of the stretches of the Zn-O bond. An AC impedance measurement of Fe<sup>3+</sup>/ZnO-400 materials was performed at 310 K using a galvanostat/potentiostat in the 50 Hz to 5.0MHz frequency range. The domain margin resistance is 26.10 MΩ and 18.10 MΩ (at room temperature, 310 K) for Fe<sup>3+</sup>/ZnO-RT and Fe<sup>3+</sup>/ZnO-400 samples, respectively.

## Acknowledgment

Authors are grateful to the Department of Physics, B.M.U., Rohtak, India for the necessary facilities.

## References

- [1]. D. Gao, et al., Room temperature ferromagnetism of pure ZnO nano particles, Journal of applied physics 105.11 (2009): 113928.
- [2]. T. Sahoo et al., Synthesis and characterization of porous ZnO nano particles by hydrothermal treatment of as pure aqueous precursor, Materials Research Bulletin 46.4 (2011): 525-530.

- [3]. S. Roy et al., Introducing magnetic properties in Fe-doped ZnO nano particles, *Applied Physics A* 127.6 (2021): 1-9.
- [4]. R. Singhal et al., Characterization of ZnO and Fe doped ZnO nano particles using fluorescence spectroscopy, *Oxide-based Materials and Devices X*. Vol. 10919. International Society for Optics and Photonics, 2019.
- [5]. C. R. Holkar et al., A critical review on textile wastewater treatments: possible approaches, *Journal of environmental management* 182 (2016): 351-366.
- [6]. A. McLaren et al., Shape and size effects of ZnO nano crystals on photo catalytic activity, *Journal of the American Chemical Society* 131.35 (2009): 12540-12541.
- [7]. M. Faraz et al., Synthesis of samarium-doped zinc oxide nano particles with improved photo catalytic performance and recyclability under visible light irradiation, *New Journal of Chemistry* 42.3 (2018): 2295-2305.
- [8]. M. Manikandan et al., Development of Sn-doped ZnO based eco friendly piezoelectric nano generator for energy harvesting application, *Nanotechnology* 31, no. 18 (2020): 185401.
- [9]. A. Akdag et al., Structural and morphological properties of Al doped ZnO nano particles, In *Journal of Physics: Conference Series*, vol. 707, no. 1, p. 012020. IOP Publishing, 2016.
- [10]. Y. Wang et al., A review of earth abundant ZnO-based materials for thermoelectric and photovoltaic applications, *Oxide-based Materials and Devices IX* 10533 (2018): 163-179.
- [8]. S. Anandan et al., Photo catalytic degradation of 2, 4, 6-trichlorophenol using lanthanum doped ZnO in aqueous suspension, *Catalysis Communications* 8.9 (2007): 1377-1382.
- [9]. Y. Sun et al., Growth of aligned ZnO nano rod arrays by catalyst-free pulsed laser deposition methods, *Chemical Physics Letters* 396.1-3 (2004): 21-26.
- [10]. Huan-Ming Xiong et al., Sono chemical synthesis of highly luminescent zinc oxide nano particles doped with magnesium (II), *Angewandte Chemie International Edition* 48.15 (2009): 2727-2731.

- [11]. U. Megha et al., Room temperature AC impedance and dielectric studies of Bi and Sr doped Pr Co<sub>0.6</sub> Fe<sub>0.4</sub>O<sub>3</sub> perovskites, *Processing and application of Ceramics* 11.1 (2017) : 52-59.
- [12]. R. Zamiri et al., Structural and dielectric properties of Al-doped ZnO nanostructures, *Ceramics International* 40.4 (2014): 6031-6036.
- [13]. A. Selmi et al., Improvement of dielectric properties of ZnO nano particles by Cu doping for tunable microwave devices, *Journal of Materials Science: Materials in Electronics* 31.21 (2020): 18664-18672.